

See discussions, stats, and author profiles for this publication at: <https://www.researchgate.net/publication/326082393>

Magnetic molecularly imprinted nanoparticles for the solid-phase extraction of diazinon from aqueous medium, followed its determination by HPLC-UV

Article · January 2017

CITATIONS

2

READS

18

3 authors, including:



Ramin Karimian

Chemical Injuries Research Center, Systems biology and poisonings institute, Baq...

32 PUBLICATIONS 155 CITATIONS

SEE PROFILE



Farideh Piri

University of Zanjan

42 PUBLICATIONS 251 CITATIONS

SEE PROFILE

Some of the authors of this publication are also working on these related projects:



nano silica [View project](#)



semi industrial production of graphene [View project](#)

Magnetic Molecularly Imprinted Nanoparticles for the Solid-Phase Extraction of Diazinon from Aqueous Medium, Followed Its Determination by HPLC-UV

Ramin Karimian^{1*}, Farideh Piri², Zahra Hosseini²

Abstract

The aim of the present work was to investigate the feasibility of employing the molecular imprinting polymer technique for detecting diazinon using magnetic molecularly imprinted nanoparticles. The magnetic molecularly imprinted nanoparticles were prepared in the presence of a template diazinon molecule. These nanoparticles exhibited a linear response in the range of 2-20 ppm ($y = 0.2634 \times C_{\text{diazinon}} - 0.0575$, $R^2 = 0.9892$) for detection of diazinon. The adsorption kinetics and isotherms and the selectivity efficiencies of diazinon and other structurally related analogues were investigated by HPLC-UV as well, respectively. The results showed that the magnetic molecularly imprinted nanoparticles have high adsorption capacity, controlled selectivity, and direct magnetic separation in aqueous environments. The results indicate that the spiked recoveries were changed from 73 to 85%, and the RSD was lower than 11.91

1. Applied Biotechnology Research Center, Baqiyatallah University of Medical Sciences, Tehran, Iran

2. Department of Chemistry, Faculty of Science, Zanjan University, Zanjan, Iran

* Corresponding Author

Ramin Karimian

Applied Biotechnology Research Center, Baqiyatallah University of Medical Sciences, Tehran, Iran
E-mail: karimian.r@gmail.com

Keywords: Magnetic Molecularly Imprinted, Nanoparticle, Diazinon, Selective Recognition, Adsorption Kinetic, Adsorption Isotherm

Submission Date: 2/22/2017

Accepted Date: 4/10/2017

Introduction

Molecular imprinting is a rapidly developing technique to prepare polymers possessing high recognition properties [1-4]. These polymers (molecularly imprinted polymer) are synthetic polymers possessing high selective molecular recognition properties because of recognition sites within the polymer matrix that are complementary to the target molecule (template) in terms of the size and positioning of functional groups. In fact, molecular imprinting is a process in which functional and cross-linking monomers are polymerized in the presence of the template. The technique relies on the formation of specific recognition sites in the synthesized polymer. First, the functional monomers interact with the template resulting in the formation of a pre-polymerization complex. Subsequently, the polymerization is initiated through 2,2'-azobisisobutyronitrile, ultraviolet light, or heat. In the presence of a cross-linking monomer, a dense polymer network is formed due to the fixation of the functional monomers around the template. Finally, the template is washed out of the imprinted polymer leaving binding sites behind, complementary in size and shape specific to the template. These recognition sites mimic the binding sites of antibodies and enzymes [5-7]. These polymers have been utilized as materials of molecular recognition and purification in many scientific and technical fields, such as solid phase extraction, chromatographic separation, membrane separations, sensors, medical diagnostics, drug release, catalysts, and so on [8-12]. Recently, a series of MIPs, such as nanomagnetic MIPs have been developed. They have displayed application prospects in biological and environmental fields, because they have unique magnetic properties and high selectivity

for the separation of target molecule that to be handled by magnetic field. Combination of competency of MIP and magnetically characteristic of magnetic nanoparticles allow the selective and one-pot separation of target molecule from the various samples [13].

Organophosphorus pesticides are used widely in agriculture to enhance food production by controlling unwanted insects and disease vectors. Diazinon is an organophosphorus pesticide that is used extensively on lettuce, almonds, citrus, cotton, turf, alfalfa, and other crops, as well as on fruit and nut orchard crops, foundations and as an urban pest control. After applying diazinon, it is often found in the surrounding soil and surface waters, as well as on the surface of plants. The excessive use of pesticides in public health and agriculture programs has caused severe environmental pollution and potential health hazards including severe acute cases of poisonings in humans and animals. Several reports were published for the determination and extraction of diazinon from aqueous media and fruit based on MIPs [14-17].

The aim of the present study was development of an optimized magnetic diazinon imprinted nanoparticles, evaluation of its binding properties for prepared samples, and pre-concentration of diazinon from aqueous media. In this study, we used HPLC-UV as a rapid, easy, affordable, and accessible method for determination of diazinon in aqueous media.

Materials and Methods

Chemicals and materials

Iron chloride, Ferric chloride, Ammonium hydroxide (25%), Methacrylic acid (MAA), Diazinon, Chlorpyrifos,

Tetraethoxysilane (TEOS), 3-(methacryloyloxy) propyl trimethoxysilane (MPS), and Ethylene glycol dimethacrylate (EGDMA) were purchased from Sigma–Aldrich (Milwaukee, USA). 2,2'-azobisisobutyronitrile (AIBN), Igepal Co-520, and Tween 80 was purchased from Acros (Geel, Belgium). All exploited solvents [Acetonitrile (ACN), Methanol, Ethanol, Cyclohexane, Acetone and Acetic acid] were of HPLC grade and were used without further treatment.

Synthesis of Fe_3O_4 NPs

Fe_3O_4 NPs were synthesized according to the previously described method [18]. Briefly, Tween 80, $FeCl_2 \cdot 4H_2O$ (0.60 g), $FeCl_3 \cdot 6H_2O$ (1.57 g), NaOH, soybean oil, and distilled water were used in the experiments. Nanoparticles were synthesized as follows: 0.60 g of $FeCl_2 \cdot 4H_2O$ and 1.57 g of $FeCl_3 \cdot 6H_2O$ in highly purified water (2 ml) and 4% Tween 80 were added into purified soybean oil (60 ml) under mechanical stirrer with 3000 rpm until obtaining a nearly clear emulsion. This solution was referred to as solution A. NaOH (0.35 g) was dissolved into water (2.5 ml) was added drop by drop into the solution A under mechanical stirrer with 2000 rpm for 2.5 h at room temperature and then the reaction mixture was filtrated. The precipitate was washed with absolute water (3×500 ml) three times to remove the unreacted chemicals. This material was calcinated in electronic oven at 220°C for 3 h.

Synthesis of the $Fe_3O_4@SiO_2$ NPs

30 mg magnetic NPs were dissolved in 11 ml cyclohexane and 2 ml of Igepal Co-520 by sonication for 10 min followed by the addition of 2 ml ammonium hydroxide and 2.5 ml TEOS sequentially. The mixture was reacted for 12 h at the room temperature under a continuous mechanical stirring. The resultant product was collected by an external magnetic field and rinsed with highly purified ethanol three times thoroughly, and dried in a vacuum.

Synthesis of $Fe_3O_4@SiO_2@MPS$ NPs

20 mg $Fe_3O_4@SiO_2$ was dissolved in 30 ml methanol by sonication for 10 min, then 0.5 ml of MPS was added drop by drop. The mixture was reacted for 48 h at the room temperature under a continuous stirring. The resultant product was collected by an external magnetic field and rinsed with methanol thoroughly and dried in a vacuum.

Synthesis of $Fe_3O_4@MIPs$ and $Fe_3O_4@NIPs$

0.2 mM of diazinon as the template and MAA (0.4 mM) as the functional monomer, were dissolved in chloroform (5 ml). The mixture was shaken in a water bath at 25°C for 12 h and then, 20 mg of $Fe_3O_4@SiO_2@MPS$ MNPs was added with shaking for 2 h. Subsequently, 0.2 mM of EGDMA and 0.5 mM of AIBN were added into the system and the mixture was sonicated in a water bath for 2 min. After sparging with nitrogen gas for 10 min to remove oxygen, system was reacted at 60°C under nitrogen gas for 24 h to complete polymerization. The template was removed by washing the polymers with pure water and methanol–acetic acid (9:1, v/v) and acetonitrile (20 ml) in turn until no diazinon was detected by an HPLC spectrophotometer. The obtained magnetic molecularly imprinted nanoparticles (MMINPs) were dried at 40°C under vacuum. For comparison, magnetic non-molecular

imprinted polymers (NMMNIPs) were prepared under the same conditions without diazinon template.

Binding experiments

Binding experiments of $Fe_3O_4@MIPs$ and $Fe_3O_4@NIPs$

In kinetic adsorption experiments, firstly 60 mg of sorbent (MIP or NIP), was regenerated [with 10 ml methanol–acetic acid (9:1, v/v), 10 ml ACN, and 5 ml deionized water] then $Fe_3O_4@MIPs$ or $Fe_3O_4@NIPs$ was added to 10 ml of 10 mg/L of diazinon solution and incubated at ordered time intervals from 0.5 to 30 min. After that, the supernatant and polymers were separated by an external magnetic field. The concentration of diazinon in the supernatants was measured by HPLC-UV analysis. The amount of diazinon bound to the $Fe_3O_4@MIPs$ or $Fe_3O_4@NIPs$ was determined by HPLC method. In the isothermal binding experiments, after regeneration of the polymer (MIP or NIP), 60 mg of them ($Fe_3O_4@MIPs$ or $Fe_3O_4@NIPs$) were added to 10 ml acetonitrile solution containing various concentrations of diazinon varying from 0.10 to 20 mg/L and incubated for 10 min at room temperature, respectively. The supernatants and polymers were separated by an external magnetic field and the concentration of diazinon in the supernatants was measured using HPLC-UV.

Specific recognition of $Fe_3O_4@MIPs$ and $Fe_3O_4@NIPs$

10 mg of $Fe_3O_4@MIPs$ or $Fe_3O_4@NIPs$ was added to the 10 ml of acetonitrile solution containing the mixture of diazinon (10 mg/L) and chlorpyrifos (10 mg/L). After incubation for 30 min at room temperature, the supernatants and polymers were separated by an external magnetic field, then the amount of diazinon and chlorpyrifos in the supernatants was measured by HPLC-UV.

Extraction of diazinon from aqueous samples

First, 60 mg $Fe_3O_4@MIPs$ was regenerated [with 10 ml methanol–acetic acid (9:1, v/v) and 10 ml ACN] and conditioned with 5 ml deionized water added into 5 ml diazinon (10 ppm). The mixed sample was shaken for 30 min and ultrasonic for 10 min to extract diazinon. The supernatants and polymers were separated by an external magnetic field. Finally, after discarding the supernatant solution, the $Fe_3O_4@MIPs$ which had absorbed the target molecule were eluted with methanol–AcOH (9:1, v/v), and the elution was collected, evaporated to dry under a stream of nitrogen, then, the residue was condensed in 5 ml of methanol–water (3:7, v/v). The concentration of diazinon was determined by HPLC-UV.

Result and Discussion

Preparation of magnetic diazinon imprinted nanoparticle

Figure 1 illustrated the principle for preparation of $Fe_3O_4@SiO_2@MIP$ particles. First, the magnetic Fe_3O_4 nanoparticles were prepared by inverse microemulsion method [18]. Then, the Fe_3O_4 particles were coated with SiO_2 to afford $Fe_3O_4@SiO_2$ particles by the sol–gel process. The silica coating can offer the magnetic nanoparticles several advantages, such as favoring the dispersion of the magnetic particles in aqueous media, protecting the $Fe_3O_4@SiO_2$ particles from leaching, and the possibility silica covering the surface of magnetic particles may provide them with a silica-like surface more easily

modified with various groups for MIP preparation. Subsequently, the polymerizable vinyl end groups were grafted to the surface of $\text{Fe}_3\text{O}_4@\text{SiO}_2$ particles to obtain vinyl-modified $\text{Fe}_3\text{O}_4@\text{SiO}_2$ particles by the sol-gel process, which made MIP more tightly grafted on the surface of the $\text{Fe}_3\text{O}_4@\text{SiO}_2$ particles. Afterwards, in the presence of diazinon (template), functional monomer (MAA), cross

linker agent (EGDMA), and the vinyl-modified $\text{Fe}_3\text{O}_4@\text{SiO}_2$ particles the polymerization occurred at the surface of vinyl-modified $\text{Fe}_3\text{O}_4@\text{SiO}_2$ particles and the $\text{Fe}_3\text{O}_4@\text{SiO}_2@\text{MIP}$ particles were collected by an external magnetic field. Diazinon was selected as the template and $\text{Fe}_3\text{O}_4@\text{SiO}_2@\text{MIP}$ nanoparticles were prepared under the same conditions without diazinon template.

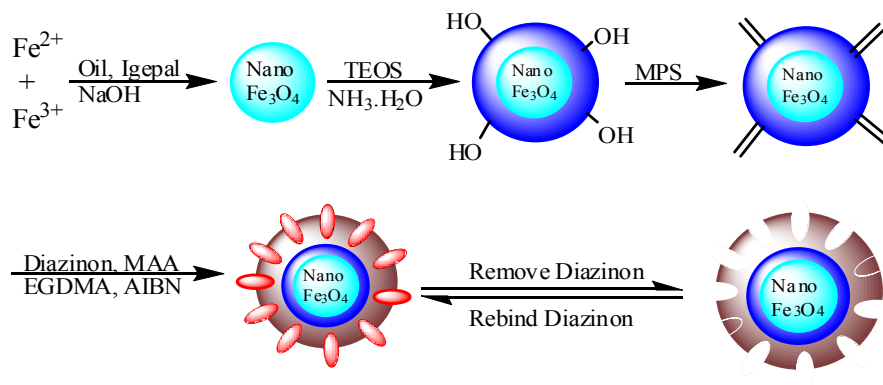


Figure 1. Scheme of preparation of $\text{Fe}_3\text{O}_4@\text{SiO}_2@\text{MIP}$.

Characterization of magnetic diazinon imprinted nanoparticles

The size and morphology of MMIP nanoparticles were measured using SEM. FT-IR spectra were recorded in the range of 4000–400/cm. The identification of the crystalline phase of MMIPs was performed using an X-ray diffractometer over the 2θ range of 10–80° [19–22].

As it can be observed in figure 2, the morphological structure and measurement of Fe_3O_4 nanoparticles, $\text{Fe}_3\text{O}_4@\text{SiO}_2$ and MIP NPs were provided by SEM and TEM. In figure 1a, the image of the Fe_3O_4 nanoparticles reveals a relatively uniform size distribution with a mean diameter of 30 nm (Fig. 2a). As illustrated in figure 2b, the $\text{Fe}_3\text{O}_4@\text{SiO}_2$ particles were approximately 35 nm in

diameter. It is obviously seen that the magnetite microspheres were uniformly dispersed in solvent. The morphology of diazinon imprinted polymer was assessed by SEM from the resulting patterns in figure 1c. It clearly showed the thickness of shell membrane of core-shell structure increases slightly.

These observations demonstrated that the MIP NPs beads had been successfully synthesized. The size of the MIP NPs was about 50 nm. So, the thickness of the imprinting layer is estimated to be about 5 nm with a relatively narrow size distribution and the MIP NPs has large and specific surface area in order to selectively adsorb the target molecules.

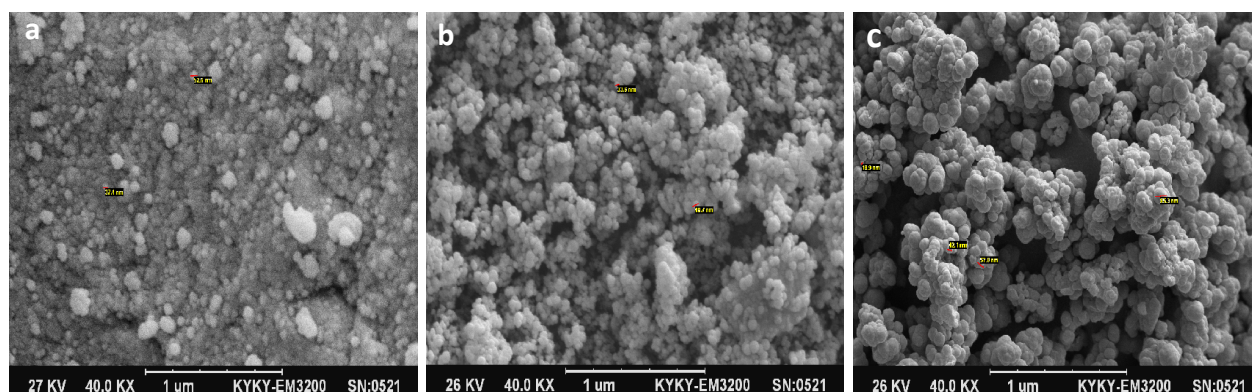


Figure 2. SEM images of Fe_3O_4 (a), $\text{Fe}_3\text{O}_4@\text{SiO}_2$ (b), and $\text{Fe}_3\text{O}_4@\text{MIP}$ NPs (c).

The products of Fe_3O_4 , $\text{Fe}_3\text{O}_4@\text{SiO}_2$, $\text{Fe}_3\text{O}_4@\text{NIPs}$ and $\text{Fe}_3\text{O}_4@\text{MIPs}$ were investigated by FT-IR spectroscopy (Fig. 3). The peak at $572/\text{cm}$ is attributed to the stretch of Fe-O (Curve A). In comparison to the infrared data of pure Fe_3O_4 , the characteristic peaks of Si-O-Si group at about $1095/\text{cm}$ and OH group at about 1621 and $3450/\text{cm}$ (Curve B) indicates the formation of silica coating on the surface of Fe_3O_4 . As it can be seen from curve C, the peaks of C-O group at $1250/\text{cm}$ and C=O group at $1730/\text{cm}$ and C-H group of methyl at $2987/\text{cm}$ indicates the methacrylic acid layer had been successfully formed on the surface of $\text{Fe}_3\text{O}_4@\text{SiO}_2$. In addition, the curves of $\text{Fe}_3\text{O}_4@\text{MIPs}$ (Curve E) and $\text{Fe}_3\text{O}_4@\text{NIPs}$ (Curve D) have almost the same characteristic peaks, which show the complete removal of templates. These results demonstrate the coatings of MIPs and NIPs on the surface $\text{Fe}_3\text{O}_4@\text{SiO}_2$ are very stable and high productivity. It was found that the band at $1024/\text{cm}$ which correspond to stretching vibration of P-O- $\text{CH}_2\text{-CH}_3$ broadened and its intensity decreased significantly (Curve E). This shows dissociation of ethoxy groups from diazinon while, new peaks appear at 1321 and $802/\text{cm}$ and the peaks of P=S group at $632/\text{cm}$.

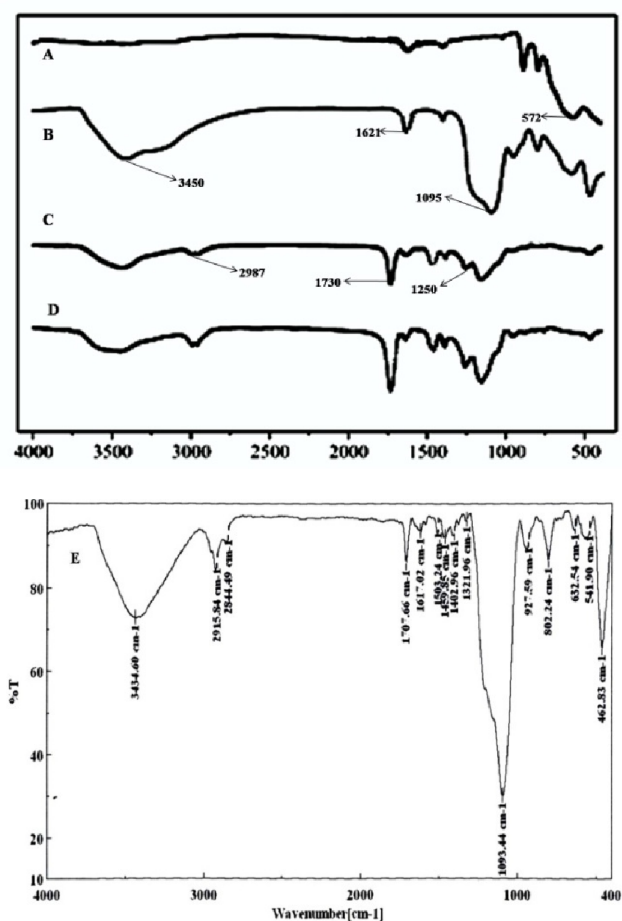


Figure 3. FT-IR spectra of Fe_3O_4 (A), $\text{Fe}_3\text{O}_4@\text{SiO}_2$ (B), $\text{Fe}_3\text{O}_4@\text{SiO}_2@\text{MPS}$ (C), $\text{Fe}_3\text{O}_4@\text{NIPs}$ (D), and $\text{Fe}_3\text{O}_4@\text{MIPs}$ (E).

The structural properties of synthesized magnetic nanoparticles were analyzed by XRD. As shown in figure 4, XRD

patterns of the synthesized Fe_3O_4 , $\text{Fe}_3\text{O}_4@\text{SiO}_2$, and magnetic diazinon imprinted nanoparticles display several relatively strong diffraction peaks in the 2 regions of $10\text{--}70^\circ$, which are quite similar to those of Fe_3O_4 MNPs reported by other groups. The discernible six diffraction peaks (30.4° , 35.5° , 43.26° , 53.63° , 57.2° , and 62.79°) in figure 4 match well with the database of magnetite in the JCPDS (JCPDS Card: 19-629) file. The XRD patterns show the presence of the specific diffraction peaks of the synthesized particles, which are highly crystalline materials. Compared with Fe_3O_4 , the intensity of these peaks decreases for $\text{Fe}_3\text{O}_4@\text{SiO}_2$ and even further for magnetic diazinon imprinted nanoparticles because of the silica coating and the MIP layer.

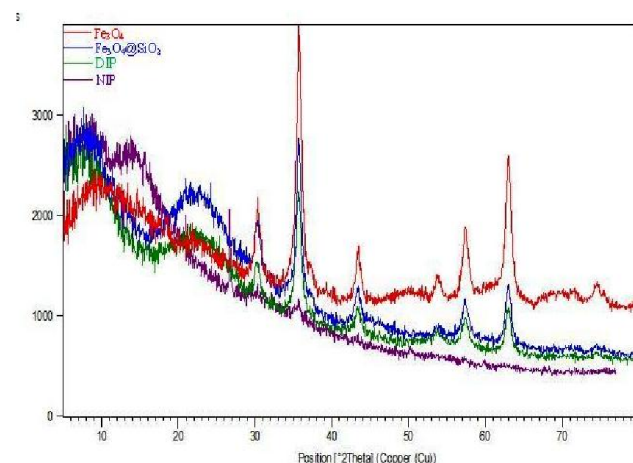


Figure 4. XRD patterns of Fe_3O_4 , $\text{Fe}_3\text{O}_4@\text{SiO}_2$, $\text{Fe}_3\text{O}_4@\text{MIP}$, and $\text{Fe}_3\text{O}_4@\text{NIPs}$.

Figure 5 shows the MIP nanoparticles have excellent magnetic properties when they are dispersed in water. When a magnet was placed beside the mixture solution, the nanoparticles moved toward the magnet and form a film on the flask wall close to the magnet, due to their magnetism.



Figure 5. Photograph of magnetic separation for MIP nanoparticles.

Binding experiments of $\text{Fe}_3\text{O}_4@\text{MIPs}$ and $\text{Fe}_3\text{O}_4@\text{NIPs}$

In kinetic adsorption experiments, firstly 60 mg of sorbent (MIP or NIP) was regenerated [with 10 ml methanol-acetic acid (9:1, v/v), 10 ml ACN and 5 ml deionized water], then $\text{Fe}_3\text{O}_4@\text{MIPs}$ or $\text{Fe}_3\text{O}_4@\text{NIPs}$ was added to 10 ml of 10 mg/L of diazinon solution and incubated at ordered time intervals from 0.5 to 30 min . After that, the

supernatant and polymers were separated by an external magnetic field. The concentration of diazinon in the supernatants was measured by HPLC-UV. The amount of diazinon bound to the Fe₃O₄@MIPs or Fe₃O₄@NIPs was determined by HPLC method.

In the isothermal binding experiment, After regeneration of polymer (MIP or NIP), 60 mg of them (Fe₃O₄@MIPs or Fe₃O₄@NIPs) were added to 10 ml acetonitrile solution of diazinon of various concentrations from 0.10 to 20 mg/L and incubated for 10 min at room temperature, respectively. The supernatants and polymers were separated by an external magnetic field, and the concentration of diazinon in the supernatant was measured by HPLC-UV.

The recognition ability of diazinon with Fe₃O₄@MIPs NPs was investigated by an adsorption kinetics test. The adsorption kinetics of 10 mg/L diazinon solution onto Fe₃O₄@MIPs and Fe₃O₄@NIPs was presented in figure 6A. The adsorption process could be divided into two steps, a quick step and a slow one. In the first step, the adsorption rate was fast, and the contact time to reach equilibrium was 180 s. In the subsequent step, the adsorption was slow to reach equilibrium. In conclusion, it can be seen that the adsorption capacity increased with time and the imprinted NPs had a fast adsorption rate. The adsorption capacity increased rapidly in the first 15 s and almost reached equilibrium after 180 s. In this work the equilibrium time of the Fe₃O₄@MIP is shorter than that of the other surface imprinting technology for diazinon. The imprinted Fe₃O₄@MIPs needs only 15–180 s to reach adsorption equilibrium for templates, which make diazinon molecules reach the surface imprinting cavities of Fe₃O₄@MIPs started the resulting Fe₃O₄@MIPs have the property of good mass transport and thus overcome some drawbacks of traditional packing imprinted materials.

The binding isotherm data obtained from MMIPs and MNIPs rebinding performance are plotted (Fig. 6B). The MMIP and MNIP toward diazinon were investigated by changing the concentration of diazinon in the range of 2 to 50 mg/L in the presence of 60 mg MMIP or MNIP at room temperature. With increasing initial diazinon concentration, the adsorption capacities increase for both MMIP and MNIP. Because of the imprinting effect, MMIP exhibits a much higher adsorption capacity than that of MNIP [23, 24]. Therefore, the maximum binding amount of MMIPs toward diazinon was much higher than that of MNIPs.

In general, the Scatchard plot is used for the evaluation of adsorption parameters and it can indicate how many kinds of binding sites exist in the MIP [25, 26] and Scatchard analysis [28] was used for evaluation of the adsorption of MMIPs and MNIPs according to Scatchard equation. The Scatchard equation is as follows:

$$\frac{Q}{C_e} = \frac{Q_{max} - Q}{K_d}$$

In above equation, Q is the amount of diazinon bound to the MMIPs or MNIPs at equilibrium, C_e is the concentration of free diazinon at equilibrium, K_d is the dissociation constant and Q_{max} is the apparent maximum binding

amount. The values of K_d and the Q_{max} can be calculated from the slope and intercept of the linear line plotted in Q/C_e versus Q.

The Scatchard plot for Fe₃O₄@MIPs was obtained. According to the Scatchard plot, adsorption was occurred uniformly on the active sites of the adsorbent. Once a template molecule occupied the site, no further adsorption could take place at this site. It was observed that the experimental data was fitted to Scatchard plot adsorption isotherm model (Fig. 6C). The adsorption process of diazinon onto Fe₃O₄@MIPs could be considered the monolayer adsorption. The linear regression equation for the linear region is Q/[diazinon] = 0.0605-0.178Q (r = 0.9239). From the slope and the intercept of the straight line obtained, the values of K_d and Q_{max} were 5.62 × 10⁻⁵ M/L and 339.89 μM/g, respectively.

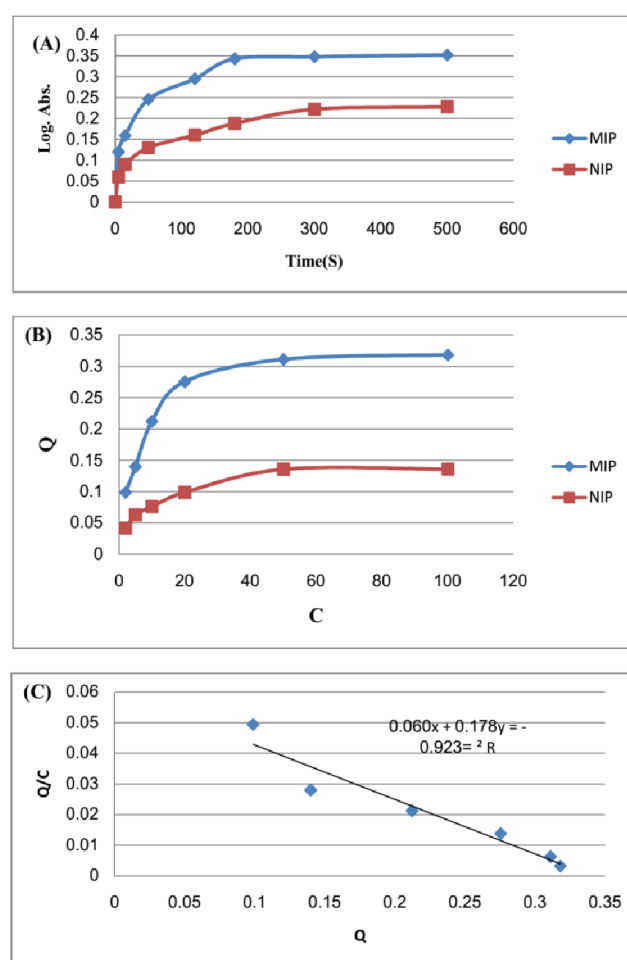


Figure 6. Adsorption kinetics of MIPs and NIP nanoparticles (A), adsorption isotherm of diazinon onto MIPs and NIP nanoparticles (B), and Scatchard analysis curves of Fe₃O₄@MIPs (C).

Selective recognition of Fe₃O₄@MIPs

To further investigate, chlorpyrifos which has similar size and structure to diazinon was chosen as the competitive species of this molecule for the selective recognition study. Distribution coefficient (K_d) and selectivity coefficient of the diazinon sorbent (k) were obtained in these competitive experiments. Distribution coefficient suggested the ratio of

the binding capacity of sorbent to the free analyses concentration in the supernatant. The selectivity coefficient of the sorbent suggested the otherness of two substances adsorbed by one sorbent, $k = K_d(\text{diazinon})/K_d(\text{chlorpyrifos})$ ($8.76/1.29 = 6.72 \approx 7$) [28, 29]. Diazinon and chlorpyrifos have the similar K_d on the NIP sorbent. The MIP sorbent shows more than seven times adsorbing capacity to diazinon than to chlorpyrifos.

Extraction of diazinon from aqueous samples

The initial experiments (before diazinon spiking) showed that there was a small amount of diazinon in aqueous media and we could not find a sample without toxin. Thus, the additional standard method was applied in calibration procedure. It means that diazinon was spiked into the aqueous medium which contained a fixed amount (X ppm) of this toxin. The standard curve was obtained from HPLC-UV analysis. Due to the low sensitivity of HPLC-UV, the minimum concentration determined in standard solutions was 2 ppm. Thus, the standard curve was also plotted in the range of 2–20 ppm. The standard calibration curve of the peak area versus the concentrations of diazinon is shown in figure 7.

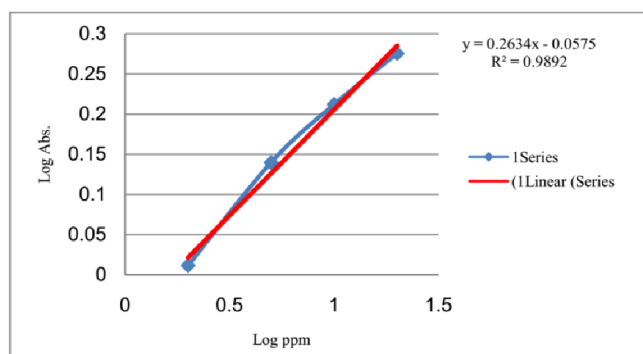


Figure 7. Linear range of the calibration curve for the diazinon at the optimized condition.

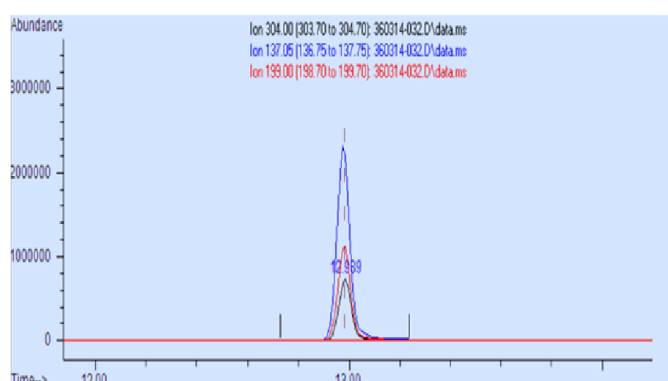


Figure 8. The GC-Mass chromatograms of a standard solution of diazinon, an aqueous sample.

The calibration plots for diazinon was linear over the concentrations range from 2 to 20 mg/L. The calibration linear equation of $y = 0.2634 \times C_{\text{diazinon}} - 0.0575$, and a linear regression coefficient (R^2) of 0.9892 were obtained in the optimal conditions. The limit of detection (LOD) is calcu-

lated on the basis of minimum distinguishable signals ($S=0.19292$) and the slope ($m=0.2634$) of the linear regression for lower concentration of template following the equation: $D.L = 3S/m$. The LOD of diazinon was obtained 2.19 mg/L. The repeatability based on the relative standard deviation (RSD%) was 11.91%. The recovery extraction of diazinon from aqueous was 73–85%. Figure 8 illustrates the chromatograms of a standard solution of diazinon, an aqueous sample with the same concentration after extraction of diazinon (three times) and GC-Mass analysis.

Conclusion

In the present study, we developed an efficient method for preparation of magnetic molecularly imprinted nanoparticles using diazinon as a template. Magnetic Fe_3O_4 nanoparticles were synthesized and the surfaces of them were successfully modified and functionalized in order to disperse in organic solvents and take part in the reaction of molecular imprinted polymerization. The obtained $\text{Fe}_3\text{O}_4@\text{MIP}$ and $\text{Fe}_3\text{O}_4@\text{NIP}$ nanoparticles were characterized by SEM, FT-IR, and XRD analyses. By this method, diazinon can be quantified in the 2-20 ppm concentration range. The recoveries for the aqueous media samples were between 73 and 85%, respectively. Besides, the adsorption behaviors, such as selective adsorption ability, adsorption kinetics, and isotherms were investigated by HPLC-UV as well. It could be concluded that the technique has great potential in developing selective extraction method for other compounds.

Acknowledgements

This study is extracted from a research project which approved and supported by applied biotechnology research center, Baqiyatallah University of Medical Sciences, Tehran, Iran.

References

1. Wulff, G., Molecular imprinting in cross-linked materials with the aid of molecular templates a way towards artificial antibodies. *Angew Chem Int Ed Engl*, 1995, Vol. 34, pp. 1812–1832.
2. Steinke, J.H.G., Sherrington, D.C., Dunkin, I.R. Imprinting of synthetic polymers using molecular templates. *Adv Polym Sci*, 1995, Vol. 123, pp. 82–125.
3. Shea, K.J., Spivak, D.A., Sellergren, B.J. Polymer complements to nucleotide bases. Selective binding of adenine derivatives to imprinted polymers. *Am Chem Soc*, 1993, Vol. 115, pp. 3368–3369.
4. Vlatakis, G., Andersson, L.I., Muller, R., Mosbach, K. Drug assay using antibody mimics made by molecular imprinting. *Nature*, 1993, Vol. 361, pp. 645–647.
5. Haupt, K., Mosbach, K. Molecularly imprinted polymers and their use in biomimetic sensors. *Chem Rev*, 2000, Vol. 100, pp. 2495–2504.
6. Haupt, K. Peer reviewed: molecularly imprinted polymers: the next generation. *Anal Chem*, 2003, Vol. 75, pp. 376A–383A.
7. Wulff, G. Enzyme-like Catalysis by Molecularly Imprinted Polymers. *Chem Rev*, 2002, Vol. 102, pp. 1–28.
8. Ge, Y., Butler, B., Mirza, F., Habib-Ullah, S. Smart molecularly imprinted polymers: recent developments and applications. *Macromol*, 2013, Vol. 34, pp. 903–915.
9. Cheong, W.J., Yang, S.H., Ali, F. Molecular imprinted polymers for separation science: a review of reviews. *J Sep Sci*, 2013, Vol. 36, pp. 609–628.

10. Najafzadeh, P., Ebrahimi, S.A. Synthesis of a phenylalanine imprinted polymer for attenuation of phenylalanine absorption via the gut in a murine hyperphenylalaninemia model. *J Mater Chem B*, 2013, Vol. 2, pp. 2144-2152.
11. Unluer, O.B., Ersoz, A., Denizli, A. Separation and purification of hyaluronic acid by embedded glucuronic acid imprinted polymers into cryogel. *J Chromatogr B*, 2013, Vol. 934, pp. 46-52.
12. Li, B., Xu, J.J., Hall, A.J., Haupt, K. Water-compatible silica sol-gel molecularly imprinted polymer as a potential delivery system for the controlled release of salicylic acid. *J Mol Recognit*, 2014, Vol. 27, pp. 559-565.
13. Lv, Y., Tan, T., Svec, F. Molecular imprinting of proteins in polymers attached to the surface of nano materials for selective recognition of biomacromolecules. *Biotechnol Adv*, 2013, Vol. 31, pp. 1172-1186.
14. Davoodi, D., Khayyat, M.H., Mohajeri, S.A., Rezaei, M.A. Preparation, evaluation and application of diazinon imprinted polymers as the sorbent in molecularly imprinted solid-phase extraction and liquid chromatography analysis in cucumber and aqueous samples. *Food Chemistry*, 2014, Vol. 158, pp. 421-428.
15. Bayat, M., Hassanzadeh-Khayyat, M., Mohajeri, S.A. Determination of diazinon pesticide residue in Tomato fruit and Tomato paste by molecularly imprinted solid-phase extraction coupled with liquid chromatography analysis. *Food Anal Methods*, 2015, Vol. 8, pp. 1034-1041.
16. Alamgir, M., Chowdhury, Z., Bhattacharjee, Sh., Fakhruddin, A.N.M., Islam, M.N., Khorshed M. Determination of cypermethrin, chlorpyrifos and diazinon residues in Tomato and reduction of cypermethrin residues in Tomato using Rice bran. *World J Agric Res*, 2013, Vol. 1, pp. 30-35.
17. Hernandez, F., Sancho, J.V., Pozo, O.J. Critical Review of the application of liquid chromatography to the determination of pesticide residues in biological samples. *Anal Bioanal Chem*, 2005, Vol. 382, pp. 934-946.
18. Karimian, R., Piri, F. Synthesis and investigation the catalytic behavior of Cr₂O₃ nanoparticles. *J Nanostruct*, 2013, Vol. 3, pp. 87-92.
19. Chen, J., Liang, R.P., Wang, X.N., Qiu, J.D. A norepinephrine coated magnetic molecularly imprinted polymer for simultaneous multiple chiral recognition. *J Chromatogr A*, 2015, Vol. 1409, pp. 268-276.
20. Hu, Y.L., Liu, R.J., Zhang, Li, G.K. Improvement of extraction capability of magnetic molecularly imprinted polymer beads in aqueous media via dual-phase solvent system. *Talanta*, 2009, Vol. 79, pp. 576-582.
21. Chen, L.G., Liu, J., Zeng, Q.L., Wang, H., Yu, A.M., Zhang, H.Q., Ding, L. Preparation of magnetic molecularly imprinted polymer for the separation of tetracycline antibiotics from egg and tissue samples. *J Chromatogr A*, 2009, Vol. 1216, pp. 3710-3719.
22. Li, Y., Li, X., Chu, J., Dong, C.K., Qi, J.Y., Yuan, Y.X. Synthesis of core-shell magnetic molecular imprinted polymer by the surface RAFT polymerization for the fast and selective removal of endocrine disrupting chemicals from aqueous solutions. *Environ Pollut*, 2010, Vol. 158, pp. 2317-2323.
23. Chen, L., Li, B. Determination of imidacloprid in rice by molecularly imprinted-matrix solid-phase dispersion with liquid chromatography tandem mass spectrometry. *J Chromatogr B*, 2012, Vol. 897, pp. 32-36.
24. Liu, Y., Huang, Y., Liu, J., Wang, W., Liu, G., Zhao, R. Superparamagnetic surface molecularly imprinted nanoparticles for water-soluble pefloxacin mesylate prepared via surface initiated atom transfer radical polymerization and its application in egg sample analysis. *J Chromatogr A*, 2012, Vol. 1246, pp. 15-21.
25. Matsui, J., Miyoshi, Y., Doblhoff-Dier, O., Takeuchi, T. A molecularly imprinted synthetic polymer receptor selective for atrazine. *Anal Chem*, 1995, Vol. 67, pp. 4404-4408.
26. Quaglia, M., Chenon, K., Hall, A.J., Lorenzi, E.D., Sellergren, B. Target Analogue Imprinted Polymers with Affinity for Folic Acid and Related Compounds. *J Am Chem Soc*, 2001, Vol. 123, pp. 2146-2154.
27. Ikegami, T., Mukawa, T., Nariai, H., Takeuchi, T. Bisphenol A-recognition polymers prepared by covalent molecular imprinting. *Anal Chim Acta*, 2004, Vol. 504, pp. 131-135.
28. Lu, Y.K., Yan, X.P. An Imprinted Organic-Inorganic Hybrid Sorbent for Selective Separation of Cadmium from Aqueous Solution. *Anal Chem*, 2004, Vol. 76, pp. 453-457.
29. Chen, D., Deng, J., Liang, J., Xie, J., Huang, K., Hu, C. Core-shell magnetic nanoparticles with surface imprinted polymer coating as a new adsorbent for solid phase extraction of metronidazole. *Anal Methods*, 2013, Vol. 5, pp. 722-728.